Supporting Information for "How does the air-sea coupling frequency affect convection during the MJO passage?"

Ning Zhao[1], Tomoe Nasuno[1]

[1]Japan Agency for Marine Earth Science and Technology, Yokosuka, Kanagawa, Japan

Contents of this file

1. Text S1 to S2
2. Figures S1 to S6
3. Table S1

Introduction There are two sections included in the supporting information. Section S1 shows the details of the sensitivity experiments for cumulus parameterizations (Table S1), and their results are presented by Figures S1 and S2. Figure S3 shows the time series of SSTs in the experiments, which mentioned in Section 4.1 of the main text. Section S2 mainly showed the additional results when the SST was increased locally within the Sumatra region (Figures S4, S5 and S6).

Text S1. For the use of Cumulus Parameterizations In this study, all the simulations were carried out based on 7-km mesh size, which is a so-called grey zone resolution that convection is partially resolved, partially sub-grid (Gerard, 2007). At this resolution, the effect of cumulus parameterization is somehow case-by-case. Therefore, we conducted

five experiments with and without cumulus parameterizations to find the best model settings for this study (CP1H, CP1HC, CP1HC2, CP1HC3, and CP1HC4, see Table S1). All five experiments were carried out by the 1-hourly WRF-ROMS coupled model.

Especially, three cumulus schemes are scale-aware schemes, which were designed for the transition zone from the classical convection-permitting (<= 4km) and mesoscale (>= 10km) regime, including the Grell-Freitas Ensemble (GFE) scheme (Grell & Freitas, 2014), the New Simplified Arakawa-Schubert (NSAS) scheme (Kwon & Hong, 2017), and the Multi-scale Kain-Fritsch (MKF) scheme (Zheng et al., 2016). Furthermore, we also tested the New Tiedtke (NT) scheme (Zhang & Wang, 2017), which is not scale-aware but includes both deep and shallow cumulus components. Since the NSAS scheme in CP1HC3 does not have the shallow convection component, which was proved to be important in simulating convection (Pilon et al., 2016), we also applied the Global/Regional Integrated Model system (GRIMs) shallow convection scheme (Hong & Jang, 2018) following Kwon and Hong (2017).

Figure S1 shows the horizontal distributions of mean precipitation rates and maximum precipitation time during the active phase of MJO (Nov. 26th -Dec. 4th) obtained by satellite and five experiments. In general, all five simulations captured the fundamental precipitation structures but with different magnitudes. However, the heavy rainfall could only be found in CP1HC and CP1HC3, but underestimated in other experiments.

Figure S2 represents the horizontal maps of the UTC time when the maximum precipitation obtained from the GSMaP and five experiments. The maximum rainfall mainly occurred in the evening (about 12:00 UTC) over the largest islands in the study domain (i.e., Sumatra Island and Kalimantan Island) and in the early morning over the seas near

the coast. Such patterns were successfully simulated in CP1H, CP1HC, and CP1HC4, but the rainfall occurred too early in CP1HC2 and CP1HC3, especially near the coast. Over the Indian Ocean, the nighttime maximum rainfall showed two band-like patterns, which is also well-simulated in CP1HC.

Text S2. Additional results for local SST In NOCPC++, we applied the daily mean SST from CP1HC in the whole domain, which affect both local and background conditions. For our own interests, we applied the higher SST only within the Sumatra region in NOCPC+ (90 110°E, 10°S 10°N; box in Figures 1 and S3), and by doing so, we could briefly evaluate the role of local SST in promoting the convection and the circulations on a larger scale.

Our results clearly showed that the increase of local SST reduced the drier bias within the Sumatra region, but the anti-cyclonic gyre-like moisture flux anomalies remained clear and strong (Figure 4h). The only two exceptions were found in the area east of the Malay Peninsula and the area near the Java Island, where the positive (moister) biases were found downstream of the Sumatra region.

Comparing with NOCPC, the increased mean SSTs enhanced the PW and moisture fluxes in NOCPC+ (Figure S4). The locally increased SST moistened the atmosphere southwest of Sumatra region, and the largest moisture anomalies appeared near the Java Island. The eastward jet-like moisture flux anomalies, associated with two cyclonic gyre-like patterns, were similar to the background conditions as showed in CP1HC (Figure 4a), but with smaller scales and magnitudes. Whats more, the locally increased SST also induced the northward moisture transport in the Southern Hemisphere, leading to the negative biases of PW. Interestingly, over the region of Andaman Sea (west of Malay

Peninsula), the atmosphere became drier than NOCPC, even the local SST was increased (see the black box in Figure S4a). As the SST increased over the entire domain (i.e., NOCPC++; Figure S4b), the aforementioned modifications remained and further be enhanced. The cyclonic gyre became much larger and stronger, although the center moved to the west of Andaman Sea inducing a small negative bias east of Malay Peninsula.

At the sea surface, the TFLX in NOCPC+ was largely increased and 32.8 W/m^2 higher than NOCPC, even the SST difference was only about 0.6 °C. As showed in Figure S5, the TFLX was mainly controlled by the latent heat flux (LH), which was one order larger than the sensible heat flux (SH). The increased LH helped the moistening of the atmospheric boundary layer and enhanced the development of deep convection (e.g., Katsumata et al., 2018), which can be seen by the reduction of negative biases in high RH from the surface to the upper troposphere (Figures 5g and 5h). However, such enhancement in moisture supply was relatively smaller in NOCPC+ due to the lower TFLX (LH), resulting in the larger negative biases of high RH (Figure 5h and 5i). Note that T2m in NOCPC+ was similar to that in highly coupled experiments or NOCPC++, consisting of the similar sensible heat fluxes found in these two experiments (Figure S5a).

Interestingly, we found that the increased local SST induced about half of the improvement in the local convection (compared to NOCPC++). For example, the low-level moisture convergence, which could be regarded as an indicator of convection, was increased about 0.25 $\times 10^{-4}$ mm/s comparing to NOCPC (Figure 12). Similar conclusion could be found from the heat and moisture budget analyses (Figure S6). Despite the similar sub-daily biases due to the lack of higher daytime SST (see the Subsection 5a), the higher local SST reduced at least half of the underestimation of moistening/heating

processes (i.e., convective activities) in the model. Note that we used the word at least, because CP1HC also underestimated the convection as suggested by the in-situ observations (Figure 3).

References

Gerard, L. (2007). An integrated package for subgrid convection, clouds and precipitation compatible with meso-gamma scales. *Quarterly Journal of the Royal Meteorological Society*, *133*(624), 711-730. doi: 10.1002/qj.58

Grell, G. A., & Freitas, S. R. (2014). A scale and aerosol aware stochastic convective parameterization for weather and air quality modeling. *Atmospheric Chemistry and Physics*, *14*(10), 5233–5250. doi: 10.5194/acp-14-5233-2014

Hong, S., & Jang, J. (2018). Impacts of shallow convection processes on a simulated boreal summer climatology in a global atmospheric model. *Asia-Pacific Journal of Atmospheric Sciences*, *54*(5), 361-370. doi: 10.1007/s13143-018-0013-3

Katsumata, M., Mori, S., Hamada, J.-I., Hattori, M., Syamsudin, F., & Yamanaka, M. D. (2018). Diurnal cycle over a coastal area of the maritime continent as derived by special networked soundings over jakarta during harimau2010. *Progress in Earth and Planetary Science*, *5*(64). doi: 10.1186/s40645-018-0216-3

Kwon, Y. C., & Hong, S.-Y. (2017). A mass-flux cumulus parameterization scheme across gray-zone resolutions. *Monthly Weather Review*, *145*(2), 583-598. doi: 10.1175/MWR-D-16-0034.1

Pilon, R., Zhang, C., & Dudhia, J. (2016). Roles of deep and shallow convection and microphysics in the mjo simulated by the model for prediction across scales. *Journal of Geophysical Research: Atmospheres*, *121*(18), 10,575-10,600. doi:

10.1002/2015JD024697

Zhang, C., & Wang, Y. (2017). Projected future changes of tropical cyclone activity over the western north and south pacific in a 20-km-mesh regional climate model. *Journal of Climate*, *30*(15), 5923-5941. doi: 10.1175/JCLI-D-16-0597.1

Zheng, Y., Alapaty, K., Herwehe, J. A., Del Genio, A. D., & Niyogi, D. (2016). Improving high-resolution weather forecasts using the weather research and forecasting (wrf) model with an updated kain-fritsch scheme. *Monthly Weather Review*, *144*(3), 833-860. doi: 10.1175/MWR-D-15-0005.1

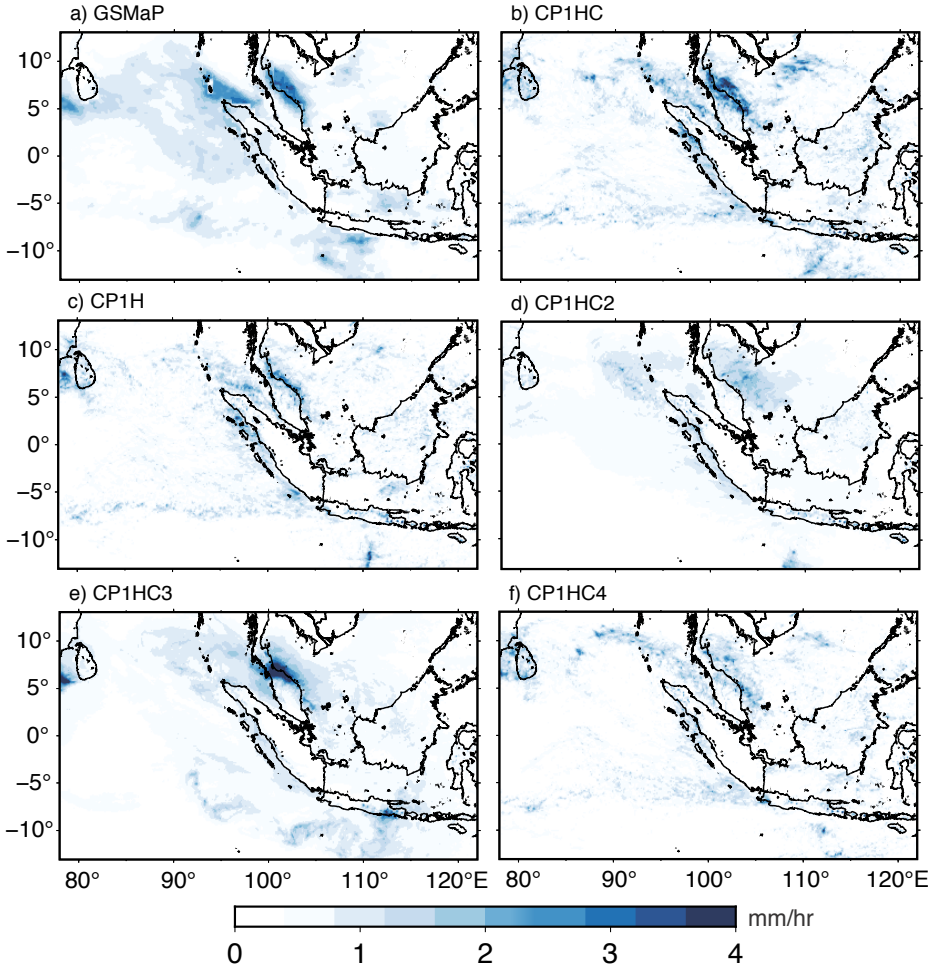

Figure S1. Horizontal distributions of the precipitation rates obtained from satellite observations and models with different cumulus parameterizations. (a) GSMaP; (b) CP1HC (GFE scheme); (c) CP1H (no cumulus scheme); (d) CP1HC2 (NT scheme); (e) CP1HC3 (NSAS + GRIMs scheme); and (f) CP1HC4 (MKF scheme). Note that, for ease to compare, panel S1a and S1b are identical to Figure 2a and 2b, respectively.

Table S1. Descriptions of the sensitivity experiments

Experiment	Cumulus Parameterization
CP1H	N/A
CP1HC	GFE scheme
CP1HC2	NT scheme
CP1HC3	NSAS + GRIMs scheme
CP1HC4	MKF scheme

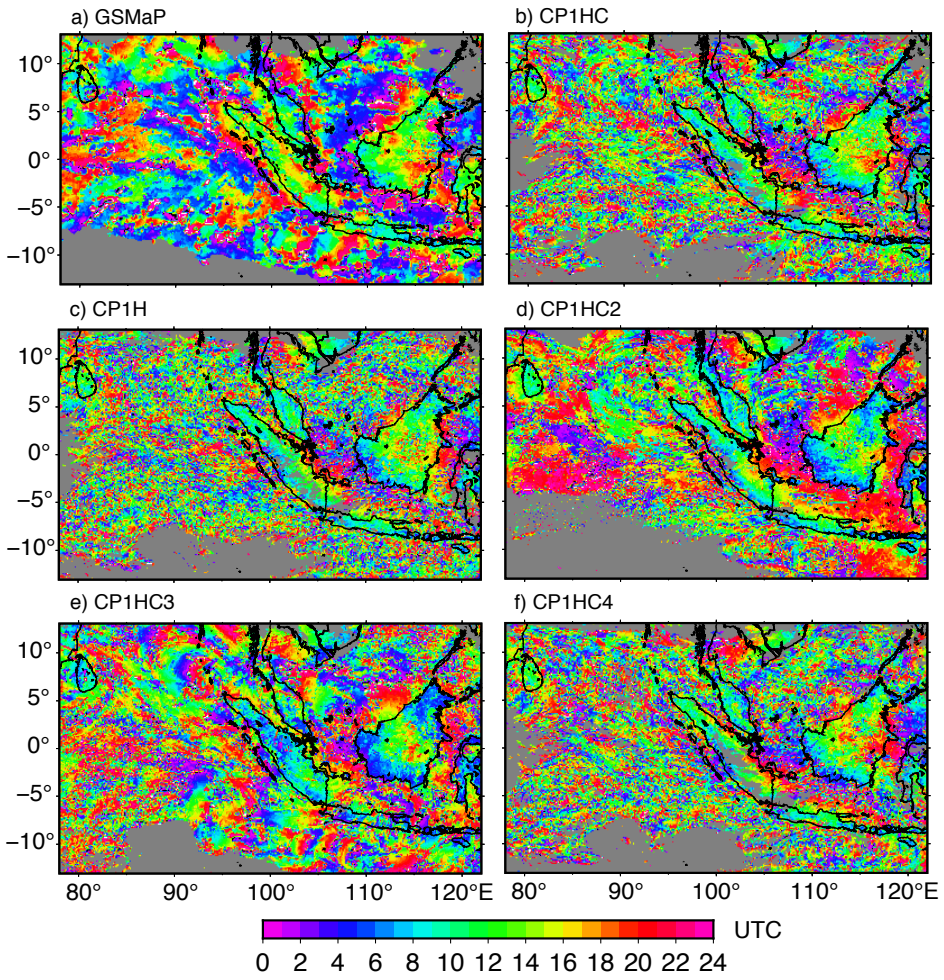

Figure S2. Same as Figure 2 but for the time of maximum precipitation (in UTC). Grids with weak precipitation (< 1 mm/hr) were excluded.

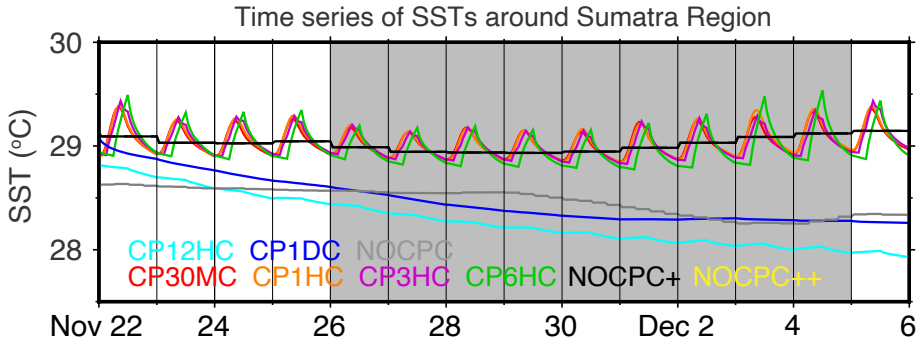

Figure S3. Same as Figure 6 but for the time series of SSTs. Note that the SSTs in NOCPC+ and NOCPC++ were identical, so that no yellow line can be seen.

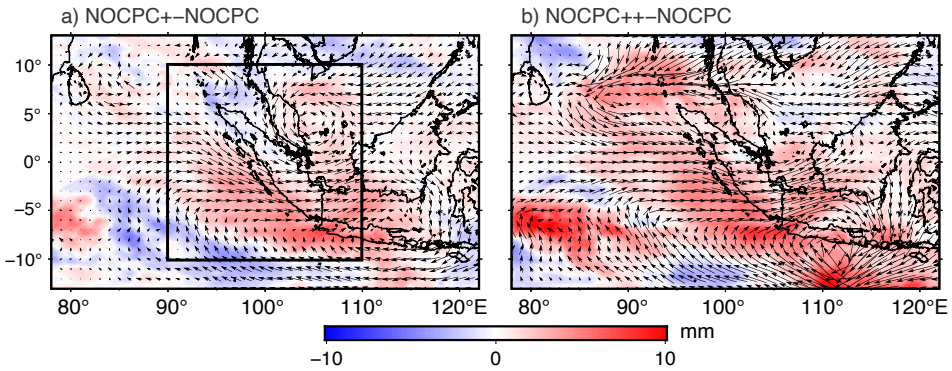

Figure S4. Improvement of the precipitable water and moisture fluxes during the active phase of MJO (November 26th to December 4th) in (a) NOCPC+ and (b) NOCPC++ in comparison with NOCPC. The Sumatra region is indicated by the black box in panel a, which is same as the red box in Figure 1.

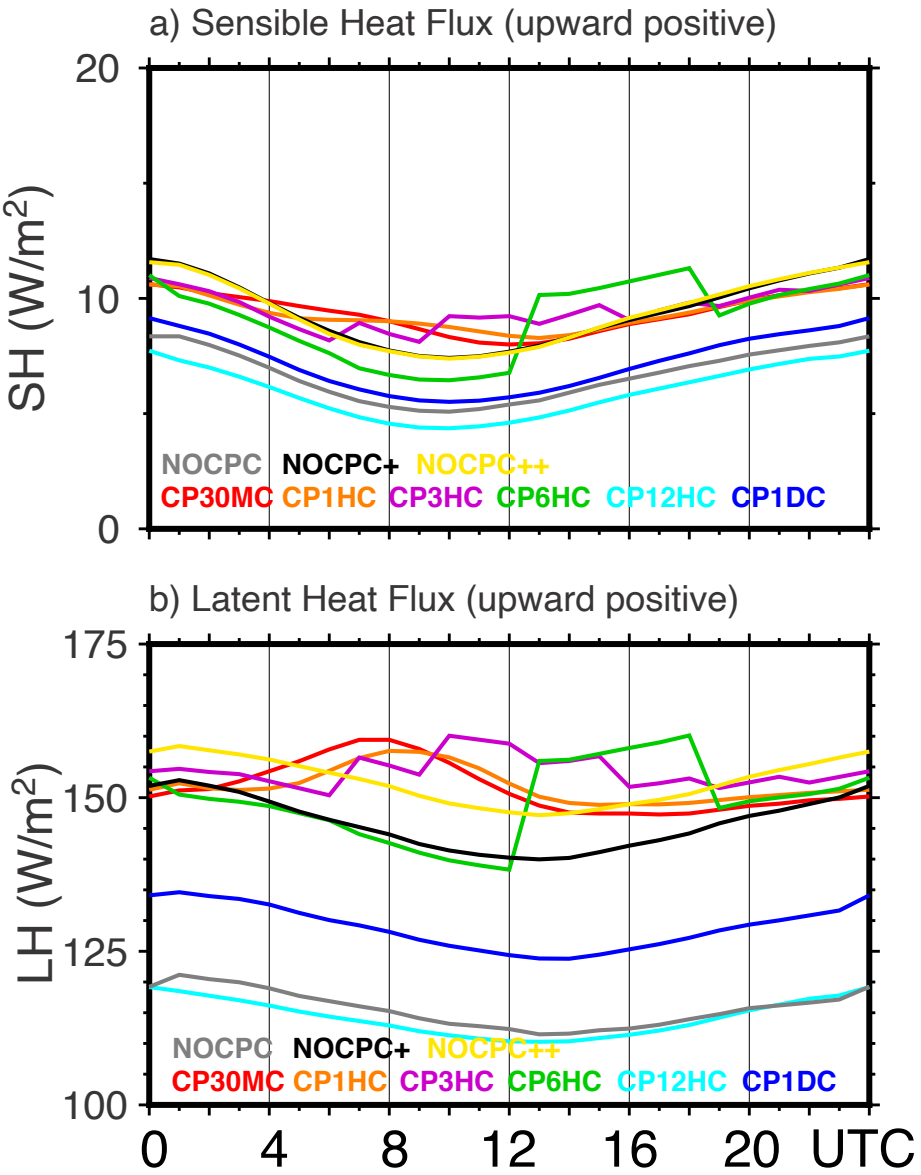

Figure S5. Diurnal composites of (a) the sensibile heat flux and (b) the latent heat flux. Positive value means atmosphere gains heat (i.e., upward positive).

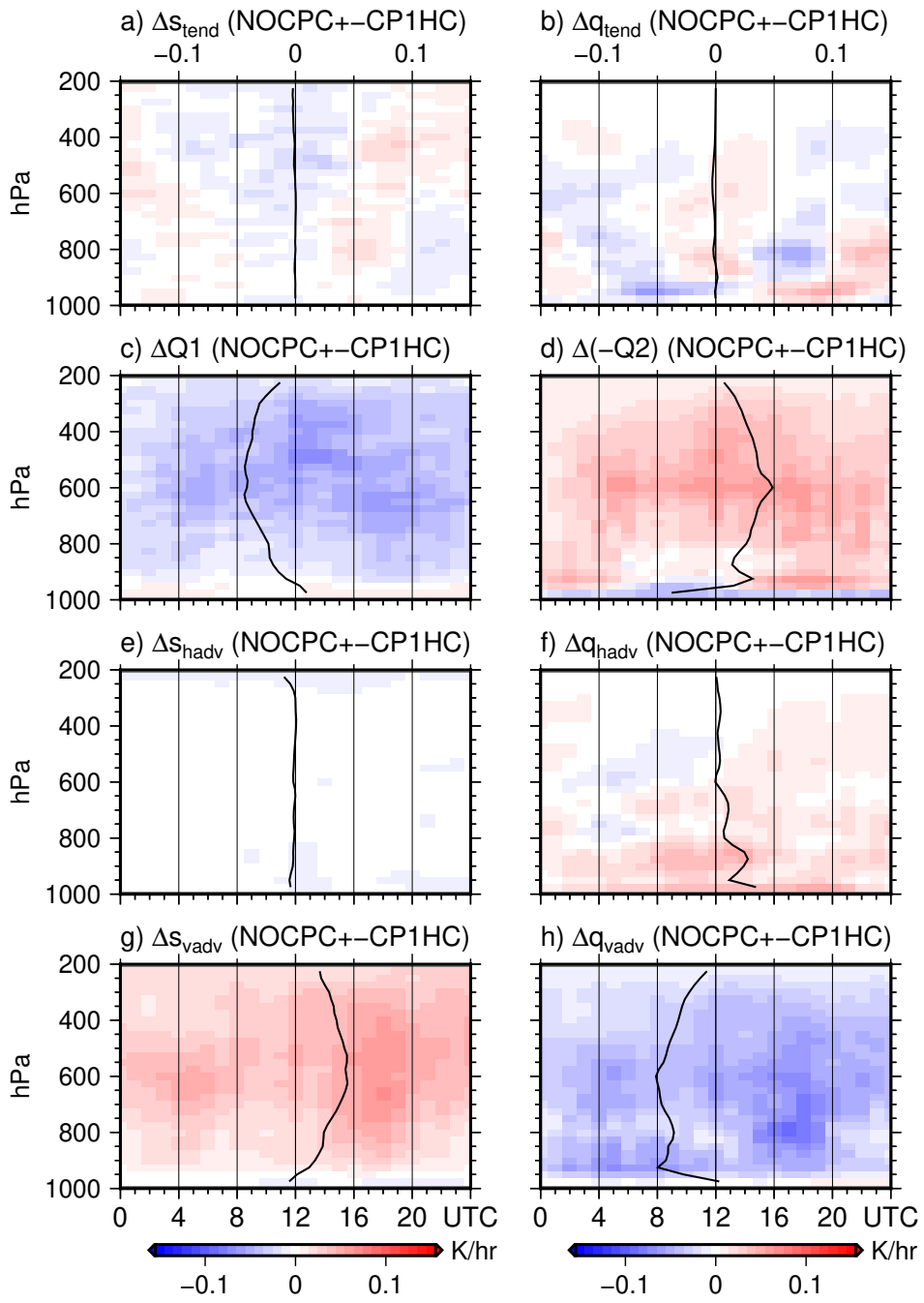

Figure S6. Diurnal composites of the differences in heat and moisture budget between NOCPC+ and CP1HC.